nature physics

ARTICLES

https://doi.org/10.1038/s41567-018-0081-4

Mutual information, neural networks and the renormalization group

Maciej Koch-Janusz[1*] and Zohar Ringel[2]

Physical systems differing in their microscopic details often display strikingly similar behaviour when probed at macroscopic scales. Those universal properties, largely determining their physical characteristics, are revealed by the powerful renormalization group (RG) procedure, which systematically retains 'slow' degrees of freedom and integrates out the rest. However, the important degrees of freedom may be difficult to identify. Here we demonstrate a machine-learning algorithm capable of identifying the relevant degrees of freedom and executing RG steps iteratively without any prior knowledge about the system. We introduce an artificial neural network based on a model-independent, information-theoretic characterization of a real-space RG procedure, which performs this task. We apply the algorithm to classical statistical physics problems in one and two dimensions. We demonstrate RG flow and extract the Ising critical exponent. Our results demonstrate that machine-learning techniques can extract abstract physical concepts and consequently become an integral part of theory- and model-building.

Machine learning has been captivating public attention lately due to groundbreaking advances in automated translation, image and speech recognition[1], game-playing[2] and achieving super-human performance in tasks in which humans excelled while more traditional algorithmic approaches struggled[3]. The applications of those techniques in physics are very recent, initially leveraging the trademark prowess of machine learning in classification and pattern recognition and applying them to classify phases of matter[4–8], study amorphous materials[9,10], or exploiting the neural networks' potential as efficient nonlinear approximators of arbitrary functions[11,12] to introduce a new numerical simulation method for quantum systems[13,14]. However, the exciting possibility of employing machine learning not as a numerical simulator, or a hypothesis tester, but as an integral part of the physical reasoning process is still largely unexplored and, given the staggering pace of progress in the field of artificial intelligence, of fundamental importance and promise.

The renormalization group (RG) approach has been one of the conceptually most profound tools of theoretical physics since its inception. It underlies the seminal work on critical phenomena[15], and the discovery of asymptotic freedom in quantum chromodynamics[16], and of the Kosterlitz–Thouless phase transition[17,18]. The RG is not a monolith, but rather a conceptual framework comprising different techniques: real-space RG[19], functional RG[20] and density matrix RG[21], among others. While all of those schemes differ quite substantially in their details, style and applicability, there is an underlying physical intuition that encompasses all of them—the essence of RG lies in identifying the 'relevant' degrees of freedom and integrating out the 'irrelevant' ones iteratively, thereby arriving at a universal, low-energy effective theory. However potent the RG idea, those relevant degrees of freedom need to be identified first[22,23]. This is often a challenging conceptual step, particularly for strongly interacting systems, and may involve a sequence of mathematical mappings to models, whose behaviour is better understood[24,25].

Here we introduce an artificial neural network algorithm iteratively identifying the physically relevant degrees of freedom in a spatial region and performing an RG coarse-graining step. The input data are samples of the system configurations drawn from a Boltzmann distribution; no further knowledge about the microscopic details of the system is provided. The internal parameters of the network, which ultimately encode the degrees of freedom of interest at each step, are optimized ('learned', in neural network parlance) by a training algorithm based on evaluating real-space mutual information (RSMI) between spatially separated regions. We validate our approach by studying the Ising and dimer models of classical statistical physics in two dimensions. We obtain the RG flow and extract the Ising critical exponent. The robustness of the RSMI algorithm to physically irrelevant noise is demonstrated.

The identification of the important degrees of freedom, and the ability to execute a real-space RG procedure[19], has not only quantitative but also conceptual significance: it allows one to gain insights into the correct way of thinking about the problem at hand, raising the prospect that machine-learning techniques may augment the scientific inquiry in a fundamental fashion.

The RSMI algorithm

Before going into more detail, let us provide a bird's eye view of our method and results. We begin by phrasing the problem in probabilistic/information-theoretic terms, a language also used in refs [26–30]. To this end, we consider a small 'visible' spatial area $\mathcal{V}$, which together with its environment $\mathcal{E}$ forms the system $\mathcal{X}$, and we define a particular conditional probability distribution $P_\Lambda(\mathcal{H}|\mathcal{V})$, which describes how the relevant degrees of freedom $\mathcal{H}$ ('dubbed hiddens') in $\mathcal{V}$ depend on both $\mathcal{V}$ and $\mathcal{E}$. We then show that the sought-after conditional probability distribution is found by an algorithm maximizing an information-theoretic quantity, the mutual information, and that this algorithm lends itself to a natural implementation using artificial neural networks. We describe how RG is practically performed by coarse-graining with respect to $P_\Lambda(\mathcal{H}|\mathcal{V})$ and iterating the procedure. Finally, we provide a verification of our claims by considering two paradigmatic models of statistical physics: the Ising model—for which the RG procedure yields the famous Kadanoff block spins—and the dimer model, whose relevant degrees of freedom are much less trivial. We reconstruct the RG flow of the Ising model and extract the critical exponent.

[1]Institute for Theoretical Physics, ETH Zurich, Zurich, Switzerland. [2]Racah Institute of Physics, Hebrew University of Jerusalem, Jerusalem, Israel.
*e-mail: maciejk@ethz.ch

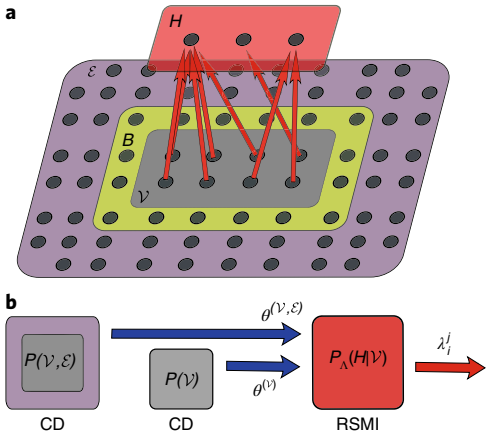

Fig. 1 | The RSMI algorithm. a, The RSMI neural network architecture. The hidden layer $\mathcal{H}$ is directly coupled to the visible layer $\mathcal{V}$ via the weights λ_i^j (red arrows). However, the training algorithm for the weights estimates mutual information between $\mathcal{H}$ and the environment $\mathcal{E}$. The buffer $\mathcal{B}$ is introduced to filter out local correlations within $\mathcal{V}$ (see Supplementary Information). **b**, The workflow of the algorithm. The CD-algorithm-trained RBMs learn to approximate probability distributions $P(\mathcal{V},\mathcal{E})$ and $P(\mathcal{V})$. Their final parameters, denoted collectively by $\Theta^{(\mathcal{V},\mathcal{E})}$ and $\Theta^{(\mathcal{V})}$, are inputs for the main RSMI network learning to extract $P_\Lambda(\mathcal{H}|\mathcal{V})$ by maximizing I_Λ. The final weights λ_i^j of the RSMI network identify the relevant degrees of freedom. They are shown in Figs. 2 and 4 for Ising and dimer problems.

Consider then a classical system of local degrees of freedom $\mathcal{X}=\{x_1,\ldots,x_N\}\equiv\{x_i\}$, defined by a Hamiltonian energy function $H(\{x_i\})$ and associated statistical probabilities $P(\mathcal{X})\propto e^{-\beta H(\{x_i\})}$, where β is the inverse temperature. Alternatively (and sufficiently for our purposes), the system is given by Monte Carlo samples of the equilibrium distribution $P(\mathcal{X})$. We denote a small spatial region of interest by $\mathcal{V}\equiv\{v_i\}$ and the remainder of the system by $\mathcal{E}\equiv\{e_i\}$, so that $\mathcal{X}=(\mathcal{V},\mathcal{E})$. We adopt a probabilistic point of view, and treat $\mathcal{X},\mathcal{E}$ and so on as random variables. Our goal is to extract the relevant degrees of freedom $\mathcal{H}$ from $\mathcal{V}$.

'Relevance' is understood here in the following way: the degrees of freedom that RG captures govern the long-distance behaviour of the theory, and therefore the experimentally measurable physical properties; they carry the most information about the system at large, as opposed to local fluctuations. We thus formally define the random variable $\mathcal{H}$ as a composite function of degrees of freedom in $\mathcal{V}$ maximizing the 'mutual information' between $\mathcal{H}$ and the environment $\mathcal{E}$. This definition, as we discuss in the Supplementary Information, is related to the requirement that the effective coarse-grained Hamiltonian be compact and short-ranged, which is a condition any successful standard RG scheme should satisfy. As we also show, it is supported by numerical results.

Mutual information, denoted by I_λ, measures the total amount of information about one random variable contained in the other[9,10,31] (thus, it is more general than correlation coefficients). It is given in our setting by:

$$I_\Lambda(\mathcal{H}:\mathcal{E})=\sum_{\mathcal{H},\mathcal{E}}P_\Lambda(\mathcal{E},\mathcal{H})\log\left(\frac{P_\Lambda(\mathcal{E},\mathcal{H})}{P_\Lambda(\mathcal{H})P(\mathcal{E})}\right) \quad (1)$$

The unknown distribution $P_\Lambda(\mathcal{E},\mathcal{H})$ and its marginalization $P_\Lambda(\mathcal{H})$, depending on a set of parameters Λ (which we keep generic at this point), are functions of $P(\mathcal{V},\mathcal{E})$ and of $P_\Lambda(\mathcal{H}|\mathcal{V})$, which is the central object of interest.

Finding $P_\Lambda(\mathcal{H}|\mathcal{V})$ that maximizes I_Λ under certain constraints is a well-posed mathematical question and has a formal solution[32].

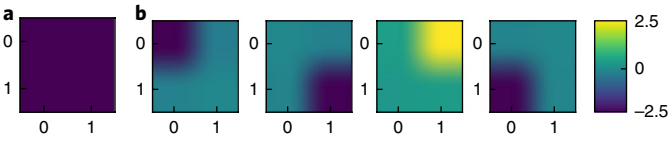

Fig. 2 | The weights of the RSMI network trained on the Ising model. Visualization of the weights of the RSMI network trained on the Ising model for a visibile area $\mathcal{V}$ of 2×2 spins. The ANN couples strongly to areas with large absolute value of the weights. **a**, The weights for $N_h=1$ hidden neuron: the ANN discovers Kadanoff blocking. **b**, The weights for $N_h=4$ hidden neurons: each neuron tracks one original spin.

However, since the space of probability distributions grows exponentially with the number of local degrees of freedom, it is, in practice, impossible to use without further assumptions for any but the smallest physical systems. Our approach is to exploit the remarkable dimensionality reduction properties of artificial neural networks[11]. We use restricted Boltzmann machines (RBMs), a class of probabilistic networks well adapted to approximating arbitrary data probability distributions. An RBM is composed of two layers of nodes, the 'visible' layer, corresponding to local degrees of freedom in our setting, and a 'hidden' layer. The interactions between the layers are defined by an energy function $E_\Theta\equiv E_{a,b,\theta}(\mathcal{V},\mathcal{H})=-\sum_j b_j h_j-\sum_i a_i v_i-\sum_{ij}v_i\theta_{ij}h_j$, such that the joint probability distribution for a particular configuration of visible and hidden degrees of freedom is given by a Boltzmann weight:

$$P_\Theta(\mathcal{V},\mathcal{H})=\frac{1}{\mathcal{Z}}e^{-E_{a,b,\theta}(\mathcal{V},\mathcal{H})} \quad (2)$$

where $\mathcal{Z}$ is the normalization. The goal of the network training is to find parameters θ_{ij} ('weights' or 'filters') and a_i,b_i optimizing a chosen objective function.

Three distinct RBMs are used. Two are trained as efficient approximators of the probability distributions $P(\mathcal{V},\mathcal{E})$ and $P(\mathcal{V})$, using the celebrated contrastive divergence (CD) algorithm[33]. Their trained parameters are used by the third network (see Fig. 1b), which has a different objective: to find $P_\Lambda(\mathcal{H}|\mathcal{V})$ maximizing I_Λ. To the end we introduce the real-space mutual information (RSMI) network, whose architecture is shown in Fig. 1a. The hidden units of RSMI correspond to coarse-grained variables $\mathcal{H}$.

The parameters $\Lambda=(a_i,b_j,\lambda_i^j)$ of the RSMI network are trained by an iterative procedure. At each iteration, a Monte Carlo estimate of function $I_\Lambda(\mathcal{H}:\mathcal{E})$ and its gradients is performed for the current values of parameters Λ. The gradients are then used to improve the values of weights in the next step, using a stochastic gradient descent procedure.

The trained weights Λ define the probability $P_\Lambda(\mathcal{H}|\mathcal{V})$ of a Boltzmann form, which is used to generate MC samples of the coarse-grained system. Those, in turn, become input to the next iteration of the RSMI algorithm. The estimates of mutual information, weights of the trained RBMs and sets of generated MC samples at every RG step can be used to extract quantitative information about the system in the form of correlation functions, critical exponents and so on, as we show below and in the Supplementary Information. We also emphasize that the parameters Λ identifying relevant degrees of freedom are re-computed at every RG step. This potentially allows RSMI to capture the evolution of the degrees of freedom along the RG flow[34].

Validation

To validate our approach, we consider two important classical models of statistical physics: the Ising model, whose coarse-grained degrees of freedom resemble the original ones, and the fully packed dimer model, where they are entirely different.

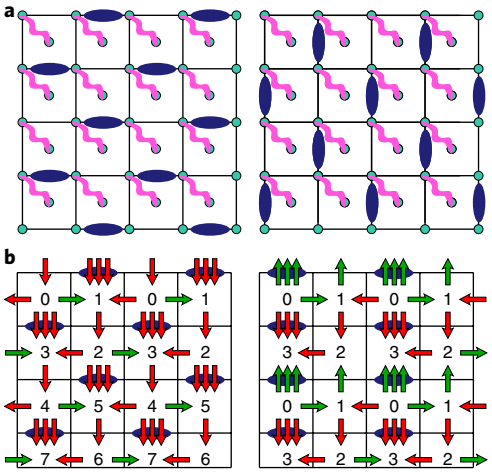

Fig. 3 | The dimer model. a, Two sample dimer configurations (blue links), corresponding to the E_y and E_x electrical fields, respectively. The coupled pairs of additional spin degrees of freedom on vertices and faces of the lattice (wiggly lines) are decoupled from the dimers and from each other. Their fluctuations constitute irrelevant noise. **b**, An example of mapping the dimer model to local electric fields. The so-called staggered configuration on the left maps to uniform non-vanishing field in the vertical direction: $\langle E_y \rangle \neq 0$. The 'columnar' configuration on the right produces both E_x and E_y that are zero on average (see ref. [36] for details of the mapping).

The Ising Hamiltonian on a two-dimensional (2D) square lattice is:

$$H_{\mathrm{I}} = \sum_{\langle i,j \rangle} s_i s_j \tag{3}$$

with $s_i = \pm 1$ and the summation over nearest neighbours. Real-space RG of the Ising model proceeds by the block-spin construction[19], whereby each 2×2 block of spins is coarse-grained into a single effective spin, whose orientation is decided by a 'majority' rule.

The results of the RSMI algorithm trained on Ising model samples are shown in Fig. 2. We vary the number of both hidden neurons N_{h} and the visible units, which are arranged in a 2D area $\mathcal{V}$ of size $L\times L$ (see Fig. 1a). For a four-spin area, the network indeed rediscovers the famous Kadanoff block-spin: Fig. 2a shows a single hidden unit coupling uniformly to four visible spins (that is, the orientation of the hidden unit is decided by the average magnetization in the area). Figure 2b is a trivial but important sanity check: given four hidden units to extract relevant degrees of freedom from an area of four spins, the networks couples each hidden unit to a different spin, as expected. In the Supplementary Information we also compare the weights for areas $\mathcal{V}$ of different size, which are generalizations of the Kadanoff procedure to larger blocks.

We next study the dimer model, given by an entropy-only partition function, which counts the number of dimer coverings of the lattice (that is, subsets of edges such that every vertex is the endpoint of exactly one edge). Figure 3a shows sample dimer configurations (and additional spin degrees of freedom added to generate noise). This deceptively simple description hides non-trivial physics[35] and correspondingly, the RG procedure for the dimer model is more subtle, since—in contrast to the Ising case—the correct degrees of freedom to perform RG on are not dimers, but rather look like effective local electric fields. This is revealed by a mathematical mapping to a 'height field' h (see Fig. 3a,b and ref. [36]), whose gradients behave like electric fields. The continuum limit of the dimer model is given by the following action:

$$S_{\mathrm{dim}}[h] = \int \mathrm{d}^2x \, (\nabla h(\mathbf{x}))^2 \equiv \int \mathrm{d}^2x \mathbf{E}^2(\mathbf{x}) \tag{4}$$

and therefore the coarse-grained degrees of freedom are low-momentum (Fourier) components of the electrical fields E_x,E_y in the x and y directions. They correspond to 'staggered' dimer configurations shown in Fig. 3a.

Remarkably, the RSMI algorithm extracts the local electric fields from the dimer model samples without any knowledge of those mappings. In Fig. 4, the weights for $N_{\mathrm{h}}=2$ and $N_{\mathrm{h}}=4$ hidden neurons, for an 8×8 area (similar to Fig. 3a), are shown: the pattern of large negative (blue) weights couples strongly to a dimer pattern

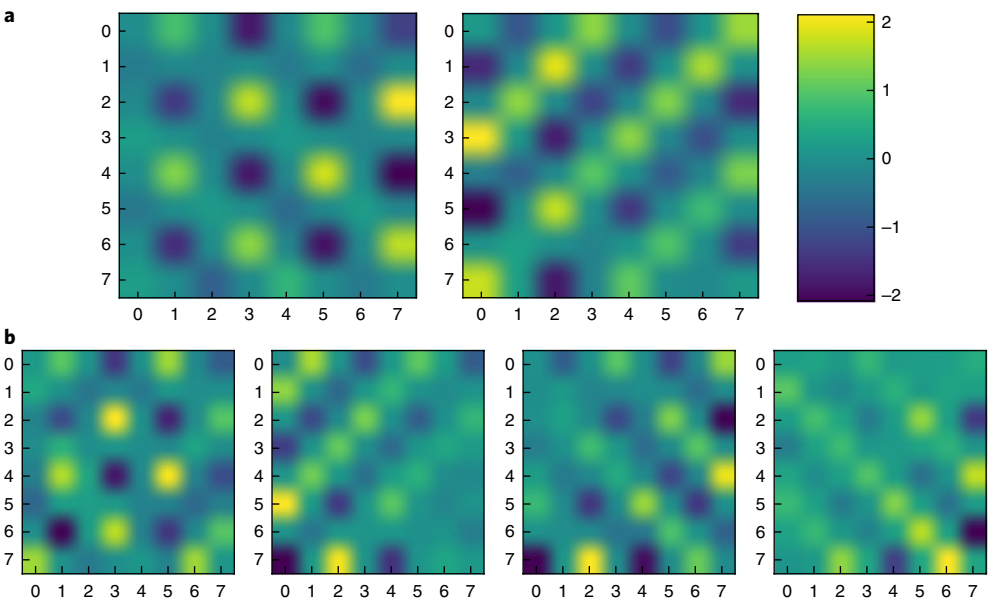

Fig. 4 | The weights of the RSMI network trained on dimer model data. a, $N_{\mathrm{h}}=2$ hidden neurons for a visible area $\mathcal{V}$ of 8×8 spins. The two filters recognize E_y and E_x+E_y electrical fields, respectively (compare with dimer patterns in Fig. 3a). **b**, The trained weights for $N_{\mathrm{h}}=4$ hidden neurons.

corresponding to local uniform E_y field (see left panels of Fig. 3a,b). The large positive (yellow) weights select an identical pattern, translated by one link. The remaining neurons extract linear superpositions $E_x + E_y$ or $E_x - E_y$ of the fields.

To demonstrate the robustness of the RSMI, we added physically irrelevant noise, forming nevertheless a pronounced pattern, which we model by additional spin degrees of freedom, strongly coupled (ferromagnetically) in pairs (wiggly lines in Fig. 3a). Decoupled from the dimers, and from other pairs, they form a trivial system, whose fluctuations are short-range noise on top of the dimer model. Vanishing weights (green in Fig. 4a,b) on sites where pairs of spins reside prove that RSMI discards their fluctuations as irrelevant for long-range physics, despite their regular pattern.

Notably, the filters obtained using our approach for the dimer model, which match the analytical expectation, are orthogonal to those obtained using Kullback–Leibler divergence. As expanded on in the Supplementary Information, this shows that standard RBMs minimizing the Kullback–Leibler divergence do not generally perform RG, thereby contradicting prior claims[37].

Finally, we demonstrate that by iterating the RSMI algorithm the qualitative insights into the nature of relevant degrees of freedom give rise to quantitative results. To this end, we revisit the 2D Ising model that (contrary to the dimer model) exhibits a non-trivial critical point at the temperature $T_c = (\log(1+\sqrt{2})/2)^{-1}$, separating the paramagnetic and ferromagnetic phases. We generate Monte Carlo samples of the system of size 128×128 at values T around the critical point, and for each one we perform up to four RG steps, by computing the Λ filters using RSMI, coarse-graining the system with respect to those filters (effectively halving the linear dimensions) and reiterating the procedure. In addition to the set of Monte Carlo configurations for the coarse-grained system, estimates of mutual information as well as the filters of the CD-trained RBMs are generated and stored. The effective temperature T of the system at each RG step can be evaluated entirely intrinsically either from correlations or the mutual information, as discussed in the Supplementary Information. Using the RBM filters, spin–spin correlations (for instance, next-nearest neighbour) can be computed. By comparing these with known analytical results[38], an additional cross-check of the effective temperature can be obtained.

In Fig. 5, the effective T is plotted against $\log_2(\xi_{128} / \xi)$, where ξ and ξ_{128} are the current and 128×128 systems' correlation lengths, respectively (this has the meaning of an RG step for integer values). The RG flow of the 2D Ising model is recovered: systems starting with $T < T_c$ flow towards ever-decreasing T (that is, an ordered state), while the ones with $T > T_c$ flow towards a paramagnet. In fact, the position of the critical point can be estimated with 1% accuracy just from the divergent flow. Furthermore, we evaluate the correlation length exponent ν, defined by $\xi \propto \tau^{-\nu}$. Using the finite-size data collapse (see Supplementary Fig. 4), its value, equal to the negative slope, is estimated to be $\nu \approx 1.0 \pm 0.15$, consistent with the exact analytical result $\nu = 1$.

Future directions

Artificial neural networks based on RSMI optimization have proved capable of extracting complex information about physically relevant degrees of freedom and using it to perform a real-space RG procedure. The RSMI algorithm we propose allows for the study of the existence and location of critical points, and RG flow in their vicinity, as well as estimation of correlations functions, critical exponents and so on. This approach is an example of a new paradigm in applying machine learning in physics: the internal data representations discovered by suitably designed algorithms are not just technical means to an end, but instead are a clear reflection of the underlying structure of the physical system (see also ref. [39]). Thus, in spite of their 'black box' reputation, the innards of such architectures may teach us fundamental lessons.

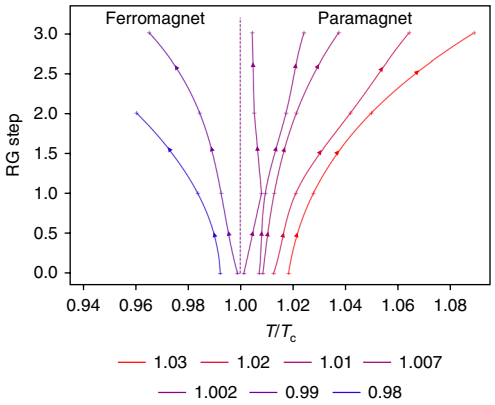

Fig. 5 | RG flow for the 2D Ising model. The temperature T (in units of T_c) as a function of the RG step for systems with initial Monte Carlo temperatures (denoted by lines of different colour) below and above T_c. See Supplementary Information for details.

This raises the prospect of employing machine learning in science in a collaborative fashion, exploiting the machines' power to distil subtle information from vast data, and human creativity and background knowledge[40].

Numerous further research directions can be pursued. Most directly, equilibrium systems with less understood relevant degrees of freedom—for example, disordered and glassy systems—can be investigated[9,10]. The ability of the RSMI algorithm to re-compute the relevant degrees of freedom at every RG step potentially allows one to study their evolution along the (more complicated) RG flow[34]. Furthermore, although we studied classical systems, the extension to the quantum domain is possible via the quantum-to-classical mapping of Euclidean path integral formalism. A more detailed analysis of the mutual-information-based RG procedure may prove fruitful from a theoretical perspective. Finally, applications of RSMI beyond physics are possible, since it offers a neural network implementation of a variant of the information bottleneck method[32], successful in compression and clustering analyses[41]; it can also be used as a local-noise-filtering pre-training stage for other machine-learning algorithms.

Data availability. The data that support the plots within this paper and other findings of this study are available from the corresponding author upon request.

Received: 11 May 2017; Accepted: 13 February 2018;
Published online: 26 March 2018

References

1. LeCun, Y., Bengio, Y. & Hinton, G. E. Deep learning. *Nature* **521**, 436–444 (2015).
2. Silver, D. et al. Mastering the game of Go with deep neural networks and tree search. *Nature* **529**, 584–589 (2016).
3. Hershey, J. R., Rennie, S. J., Olsen, P. A. & Kristjansson, T. T. Super-human multi-talker speech recognition: A graphical modeling approach. *Comput. Speech Lang.* **24**, 45–66 (2010).
4. Carrasquilla, J. & Melko, R. G. Machine learning phases of matter. *Nat. Phys.* **13**, 431–434 (2017).
5. Torlai, G. & Melko, R. G. Learning thermodynamics with Boltzmann machines. *Phys. Rev. B* **94**, 165134 (2016).
6. van Nieuwenburg, E. P. L., Liu, Y.-H. & Huber, S. D. Learning phase transitions by confusion. *Nat. Phys.* **13**, 435–439 (2017).
7. Wang, L. Discovering phase transitions with unsupervised learning. *Phys. Rev. B* **94**, 195105 (2016).
8. Ohtsuki, T. & Ohtsuki, T. Deep learning the quantum phase transitions in random electron systems: applications to three dimensions. *J. Phys. Soc. Jpn* **86**, 044708 (2017).

9. Ronhovde, P.et al Detecting hidden spatial and spatio-temporal structures in glasses and complex physical systems by multiresolution network clustering. *Eur. Phys. J. E* **34,** 105 (2011).
10. Ronhovde, P.et al Detection of hidden structures for arbitrary scales in complex physical systems. *Sci. Rep.* **2,** 329 (2012).
11. Hinton, G. E. & Salakhutdinov, R. R. Reducing the dimensionality of data with neural networks. *Science* **313**, 504–507 (2006).
12. Lin, H. W. & Tegmark, M. Why does deep and cheap learning work so well? *J. Stat. Phys.* **168**, 1223–1247 (2017).
13. Carleo, G. & Troyer, M. Solving the quantum many-body problem with artificial neural networks. *Science* **355**, 602–606 (2017).
14. Deng, D.-L., Li, X. & Sarma, S. D. Machine learning topological states. *Phys. Rev. B* **96**, 195145 (2017).
15. Wilson, K. G. The renormalization group: Critical phenomena and the Kondo problem. *Rev. Mod. Phys.* **47**, 773–840 (1975).
16. Politzer, H. D. Reliable perturbative results for strong interactions? *Phys. Rev. Lett.* **30**, 1346–1349 (1973).
17. Berezinskii, V. L. Destruction of long-range order in one-dimensional and two-dimensional systems having a continuous symmetry group I. Classical systems. *Sov. J. Exp. Theor. Phys.* **32**, 493 (1971).
18. Kosterlitz, J. M. & Thouless, D. Ordering, metastability and phase transitions in two-dimensional systems. *J. Phys. C* **6**, 1181 (1973).
19. Kadanoff, L. P. Scaling laws for Ising models near *T*(c). *Physics* **2**, 263–272 (1966).
20. Wetterich, C. Exact evolution equation for the effective potential. *Phys. Lett. B* **301**, 90–94 (1993).
21. White, S. R. Density matrix formulation for quantum renormalization groups. *Phys. Rev. Lett.* **69**, 2863–2866 (1992).
22. Ma, S.-k, Dasgupta, C. & Hu, C.-k Random antiferromagnetic chain. *Phys. Rev. Lett.* **43**, 1434–1437 (1979).
23. Corboz, P. & Mila, F. Tensor network study of the Shastry–Sutherland model in zero magnetic field. *Phys. Rev. B* **87**, 115144 (2013).
24. Capponi, S., Chandra, V. R., Auerbach, A. & Weinstein, M. *p*6 chiral resonating valence bonds in the kagome antiferromagnet. *Phys. Rev. B* **87**, 161118 (2013).
25. Auerbach, A. *Interacting Electrons and Quantum Magnetism* (Springer, New York, NY, 1994).
26. Gaite, J. & O'Connor, D. Field theory entropy, the *h* theorem, and the renormalization group. *Phys. Rev. D* **54**, 5163–5173 (1996).
27. Preskill, J. Quantum information and physics: some future directions. *J. Mod. Opt.* **47**, 127–137 (2000).
28. Apenko, S. M. Information theory and renormalization group flows. *Phys. A* **391**, 62–77 (2012).
29. Machta, B. B., Chachra, R., Transtrum, M. K. & Sethna, J. P. Parameter space compression underlies emergent theories and predictive models. *Science* **342**, 604–607 (2013).
30. Beny, C. & Osborne, T. J. The renormalization group via statistical inference. *New. J. Phys.* **17**, 083005 (2015).
31. Stephan, J.-M., Inglis, S., Fendley, P. & Melko, R. G. Geometric mutual information at classical critical points. *Phys. Rev. Lett.* **112**, 127204 (2014).
32. Tishby, N., Pereira, F. C. & Bialek, W. The information bottleneck method. In *Proc. 37th Allerton Conf. on Communication, Control and Computation* (eds Hajek, B. & Sreenivas, R. S.) **49**, 368–377 (University of Illinois, 2001).
33. Hinton, G. E. Training products of experts by minimizing contrastive divergence. *Neural Comput.* **14**, 1771–1800 (2002).
34. Ludwig, A. W. W. & Cardy, J. L. Perturbative evaluation of the conformal anomaly at new critical points with applications to random systems. *Nucl. Phys. B* **285**, 687–718 (1987).
35. Fisher, M. E. & Stephenson, J. Statistical mechanics of dimers on a plane lattice. II. Dimer correlations and monomers. *Phys. Rev.* **132**, 1411–1431 (1963).
36. Fradkin, E. *Field Theories of Condensed Matter Physics* (Cambridge Univ. Press, Cambridge, 2013).
37. Mehta, P. & Schwab, D. J. An exact mapping between the variational renormalization group and deep learning. Preprint at abs/1410.3831 (2014).
38. McCoy, B. M. & Wu, T. T. *The Two-Dimensional Ising Model* (Harvard Univ. Press, Cambridge, MA, 1973).
39. Schoenholz, S. S., Cubuk, E. D., Sussman, D. M., Kaxiras, E. & Liu, A. J. A structural approach to relaxation in glassy liquids. *Nat. Phys.* **12**, 469–471 (2016).
40. Jordan, M. I. & Mitchell, T. M. Machine learning: Trends, perspectives, and prospects. *Science* **349**, 255–260 (2015).
41. Slonim, N. & Tishby, N. Document clustering using word clusters via the information bottleneck method. In *Proc. 23rd Annual International ACM SIGIR Conf. on Research and Development in Information Retrieval*, *SIGIR '00* 208–215 (ACM, 2000).

Acknowledgements

We thank S. Huber and P. Fendley for discussions. M.K.-J. gratefully acknowledges the support of the Swiss National Science Foundation. Z.R. was supported by the European Union's Horizon 2020 research and innovation programme under the Marie Sklodowska-Curie grant agreement no. 657111.

Author contributions

M.K.-J. and Z.R. contributed equally to this work.

Competing interests

The authors declare no competing interests.

Additional information

Supplementary information is available for this paper at https://doi.org/10.1038/s41567-018-0081-4.

Reprints and permissions information is available at www.nature.com/reprints.

Correspondence and requests for materials should be addressed to M.K.

Publisher's note: Springer Nature remains neutral with regard to jurisdictional claims in published maps and institutional affiliations.